Fredrick K. Saah[1], Garima Nagpal[1], Flomo L. Gbawoquiyq[1], Rashi Chaudhary[2]*

[1]*Sharda School of Basic Sciences & Research, Department of Environmental Sciences, Sharda University, Greater Noida, Uttar Pradesh, India,* [2]*Sharda School of Basic Sciences & Research, Department of Life Sciences, Sharda University, Greater Noida, Uttar Pradesh, India*

Scientific paper
ISSN 0351-9465, E-ISSN 2466-2585
https://doi.org/10.62638/ZasMat1185

Zastita Materijala 65 (3)
440 – 451 (2024)

Groundnut shell carbon quantum dot magnetic iron oxide nanocomposite (GSCQD-$FeFe_2O_4$) for lead removal from water

ABSTRACT

A novel adsorbent, GSCQD-$FeFe_2O_4$, combining groundnut shell-derived carbon quantum dots with magnetic iron oxide nanoparticles, was synthesized for efficient removal of Pb(II) from water. Characterization studies confirmed successful synthesis, with UV analysis showing absorption at 210 nm and green luminescence indicating carbon quantum dots. FT-IR identified characteristic functional groups, while XRD confirmed well-ordered structures. FE-SEM revealed clustered carbon nanoparticles with magnetic iron oxide, and TEM showed small-sized carbon dots suitable for adsorption. Batch adsorption studies revealed optimal conditions for Pb(II) removal, including a pH range of 5-6, temperature of 20°C, contact time of 20 minutes, and adsorbent dose of 0.2 g. Isotherm studies indicated that both Langmuir and Freundlich models provided a good fit, with a calculated adsorption capacity of 37.8 mg/g. Thermodynamic analysis suggested spontaneous, exothermic adsorption with increased disorder. GSCQD-$FeFe_2O_4$ displayed excellent potential for Pb(II) removal, but further research on reusability and stability in industrial settings is needed for broader applicability.

Keywords: *carbon quantum dots, groundnut shell, magnetic iron oxide nanoparticle, lead, adsorption capacity, thermodynamic parameters, thermodynamic isotherms*

1. INTRODUCTION

Water pollution by heavy metals presents a significant global challenge due to its severe implications for human health. Safeguarding access to safe and clean drinking water is paramount, necessitating innovative approaches to combat heavy metal contamination. Ironically, human activities predominantly contribute to this pollution, raising grave health concerns [1,2]. As heavy metal concentrations exceed WHO-recommended thresholds, they infiltrate the food chain via biomanification, perpetuating human exposure [3,4]. This contamination profoundly impacts biodiversity and nutrient cycles within ecosystems, with documented detrimental effects on human health [5].

Lead, among various heavy metals occurring naturally in the environment, poses substantial health risks, particularly to children and pregnant women, even at low concentrations. Anthropogenic activities such as mining and industrial processes discharge lead into the environment, prompting the WHO to set a provisional guideline of 10 µg/L for lead (Pb(II)) in drinking water due to its toxicity and persistence [6,7]. Notably, no safe level of Pb(II) in drinking water has been established.

Numerous research endeavors have explored lead removal and decontamination technologies, prioritizing nanotechnology over conventional methods due to its superior efficacy and efficiency. Nanoadsorbents, especially those composed of composite materials, demonstrate remarkable potential in binding heavy metals in water and facilitating their removal [8,9]. Current trends emphasize the development of nanoadsorbents from sustainable sources [10].

Aligned with this approach, this study employed carbon quantum dots (CQDs) and magnetic iron oxide nanoparticles to form a composite material for the removal of Pb(II) from water. CQDs,

*Corresponding author: Garima Nagpal
Email: garima.nagpal@sharda.ac.in
Paper received: 10. 02. 2024.
Paper corrected: 26. 02. 2024.
Paper accepted: 13. 04. 2024.
Paper is available on the website: www.idk.org.rs/journal

characterized by their large surface area, stability, tunable surface chemistry, biocompatibility, and non-toxic nature, were synthesized from groundnut shells (GSCQD) due to their abundant carbon content and specific biomolecular composition of groundnut shell [11, 12, 13]. Magnetic iron oxide nanoparticles (ferrites) were chosen for their magnetic properties, extensive surface area, and versatile surface chemistry, making them efficient adsorbents for various applications. The combination of GSCQD and $FeFe_2O_4$ synergistically enhances heavy metal removal through adsorption.

The resultant GSCQD-$FeFe_2O_4$ nanocomposite, characterized by its cost-effectiveness, efficiency, and environmental friendliness, was utilized for Pb(II) removal from water. Specific operational parameters were meticulously considered, and batch studies, alongside thermodynamic parameters and adsorption isotherms, were employed to succinctly communicate the study's findings.

2. MATERIALS AND METHOD

Groundnut shells were used as carbon precursor for this research. The administrative department of Sharda University procured the necessary chemicals (from SRL) essential for this study, which included sodium hydroxide {NaOH}, hydrochloride acid {HCl}, ferric sulphate heptahydrate {$FeSO_4 \cdot 7H_2O$}, and lead nitrate {$Pb(NO_3)_2$}. Aqueous solutions were meticulously prepared using double distilled water, and the pH of the solutions was accurately adjusted with a pH meter, adding NaOH solution to obtain a basic solution or HCl for an acidic solution.

2.1. Synthesis Procedures

2.1.1. Synthesis of Groundnut Shell Carbon Quantum Dots

Multiple steps are involved in synthesizing carbon quantum dot from groundnut shells, as outlined in a study conducted by Surendran et. al., (2020) [14]. Groundnut shells are first thoroughly washed and then sun-dried. The sun-dried groundnut shells are carbonized at 70°C for 4 hours in a Muffle Furnace. After the carbonization process, the groundnut shells are ground into a fine powder. 2.0 g of the groundnut shell powder (yielded carbon) and 2.0 g of citric acid are mixed with 30 ml of distilled water. Sodium hydroxide solution is slowly added to the mixture until the pH reaches 7. The resulting solution is transferred to a Teflon-lined stainless-steel autoclave and heated at 200°C for 6 hours. After the 6-hour reaction, the autoclave can cool naturally at room temperature. The reaction solution is then subjected to 50 minutes of ultrasonication to disperse the contents. The solution is centrifuged at 5000 rpm for 1 hour under ambient conditions. The liquid portion above the sediment containing the carbon quantum dots was collected for further characterization. Fig. 1(a) showed the day light color of the liquid carbon quantum dot while Fig. 1 (b) showed the green color at short wavelength.

These steps outline the process of creating carbon quantum dot from groundnut shells, ultimately resulting in a solution of CQDs ready for further analysis and applications.

2.1.2. Synthesis of Magnetic Iron Oxide (Ferrite) nanoparticles

The procedure for synthesizing magnetic iron oxide nanoparticles follows the steps outlined in a research paper authored by Dinh et. al., (2019) [15]. A precise quantity of $FeSO_4 \cdot 7H_2O$, weighing 6.975 g, is dissolved in 141 ml of distilled water and agitated for half an hour. Subsequently, NaOH is gradually introduced into the solution while stirring to raise the pH level to 11. The mixture undergoes high-speed agitation at a rate of 1000 rpm for five hours, transforming the reaction solution from light blue to brown-black coloration. Following this step, residual moisture is eliminated by drying the mixture at a temperature of 100^{o}C for eight hours, forming a black magnetic substance known as $FeFe_2O_4$.

2.1.3. Coupling of Magnetic Iron Ferrite Nanoparticles with Groundnut Shell-Derived Carbon Quantum Dots.

The nanocomposite was synthesized following the procedure described in a research paper authored by Asadollahzadeh et al., (2021) [16]. To create a hybrid material of $FeFe_2O_4$-GSCQD nanocomposite, 200 mg of $FeFe_2O_4$ nanoparticles were mixed with 10 mg of GSCQD. The mixture was shaken overnight and then centrifuged to collect the resulting $FeFe_2O_4$-GSCQD nanocomposites. These hybrid composites were named as such for better readability.b)

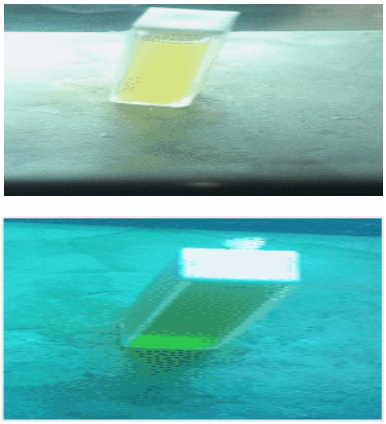

a)

b)

Figure 1. (a) Day Light Color of CQD, (b) Green color at short wavelength

2.2. Characterization

The research employed several techniques to analyze the absorbent. These include the X-Ray Diffractometer (Panalytical X Pert Pro) for analyzing the crystal structure, LAMBDA 750 (Perkin Elmer) UV-Vis NIR Spectrophotometer for determining the adsorption spectrum, field emission scanning electron microscopy (FESEM-Nova Nano FE-SEM 450 (FEI)) for capturing surface images, and transmission electron microscopy (The Tecnai G2 20 S-TWIN [FEI) is a 200 Kv TEM) for examining the morphology of the absorbent. Fourier transform infrared spectro-photometry (FT-IR Spectrum 2 (Perkin Elmer)) was also utilized to identify the functional groups present on the adsorbents.

2.3. Preparation of lead stock solution

The preparation of the lead stock solution aligns with the methodology specified in a paper written by Malacas et al. (2019) [17]. A stock solution of lead with precise concentrations was prepared. To achieve this, 1598 mg of $Pb(NO_3)_2$ were dissolved in 1000 ml of distilled water within a 1000 ml glass beaker. This resulted in the production of a 1000 ppm Pb(II) stock solution, containing exactly 1000 mg of Pb(II) for every 1000 ml of the solution. To prepare lead solutions of varying concentrations for analytical or laboratory purposes, it's necessary to use graduated cylinders and other suitable glassware. The stock solution can be diluted to achieve the desired concentration, optimizing as necessary to meet specific experimental requirements.

2.4. Batch mode adsorption and analytical procedures

This study investigates the adsorption of Pb(II) ions onto GSCQD-$FeFe_2O_4$ adsorbent. Experimental parameters were optimized, including pH, contact time, adsorbent dosage, temperature, and initial concentration. The experiments are conducted in 50 ml Erlenmeyer flasks with different parameter values. The pH of the solution varied from 3 to 9 using HCl and NaOH to adjust as required. A constant sample volume of 50 mL was used for all experiments. The contact time varies between 10 to 40 minutes, while the GSCQD-$FeFe_2O_4$ adsorbent dosage varies from 0.1 to 0.4 g. Initial lead concentrations from 10 mg/L to 70 mg/L, a temperature range of 20-35^oC, were studied precisely. Aqueous solutions of varying pH, ion concentrations, and experimental conditions were prepared to start adsorption. The GSCQD-$FeFe_2O_4$ nanocomposite adsorbents added to each Erlenmeyer flask containing the aqueous solution were agitated continuously at a speed of 200 rpm for the duration of each experiment. After a specified period, the solutions reached equilibrium. At this point, the GSCQD-$FeFe_2O_4$ nanocomposite was isolated from the solution by filtration. Subsequently, the remaining Pb(II) concentrations in the solution were determined using atomic absorption spectroscopy (AAS). The adsorption efficiency, often expressed as the percentage of Pb(II) ions removed from the solution, and the uptake capacity (represented as q_e, measured in mg/g) was calculated using the following equations or similar equations

$$q_e = (C_0 - C_e) * V/M \quad (1)$$

whereas the percentage of the uptake is given as:

$$\%\, Removal = \frac{C_0 - C_e}{C_0} * 100 \quad (2)$$

where q_e is the adsorbed amount of ions per unit mass of the adsorbent, C_0 is the initial concentration (mg/L), C_e is the equilibrium concentration of lead (mg/L), V is the volume (L) of the solution, and M is the mass of GSCQD-$FeFe_2O_4$ magnetic nanocomposite (g).

3. RESULTS AND DISCUSSION

3.1. Fourier-transform infrared spectroscopy (FTIR)

The FT-IR was used to identify the functional groups of the GSCQD (Fig. 2(a)) and GSCQD-$FeFe_2O_4$ (Fig. 2(b)) by analyzing the range of 4100-400 cm^{-1} for liquid samples in KBr cells and solid samples in KBr pellets. The analysis revealed specific critical peaks such as 1020 cm^{-1} (C-O bond), 1381 cm^{-1} (C-H bond), 1585 cm^{-1} (C=C bond), 3300 cm^{-1} (OH bond), and 582 cm^{-1} (Fe-O bond). The findings of this study are consistent with a previous study conducted by Asadollahzadeh et al., (2021) [16]. The nanocomposite of magnetic iron oxide and groundnut shell carbon quantum dots was found to have multiple functional groups. The Fe-O bond indicates the presence of magnetic iron oxide, making it suitable for use in medical, environmental, and catalytic applications. The C-O bond represents oxygen-containing groups that affect the material's reactivity and surface properties. The C-H bond is typical of organic compounds and adds to the material's stability. The C=O is part of the carbonyl functional group, which is common in various organic compounds, making the CQD more chemically reactive. The OH groups, which contain oxygen and hydrogen, contribute to the material's hydrophilicity and chemical reactions.

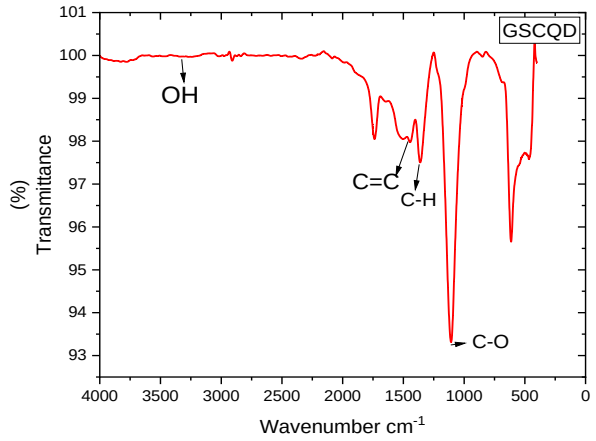

Figure 2(a) FTIR spectra of GSCQD

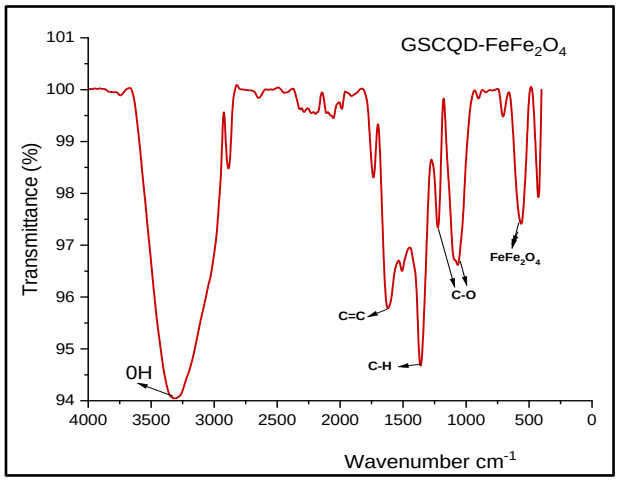

Figure 2(b) FTIR spectra of GSCQD-$FeFe_2O_4$

3.2. UV Analysis

The UV-visible absorption spectrum of GSCQD was analyzed using a LAMBDA 750 UV-Vis NIR spectrophotometer (Perkin Elmer), as shown in Figure 3.

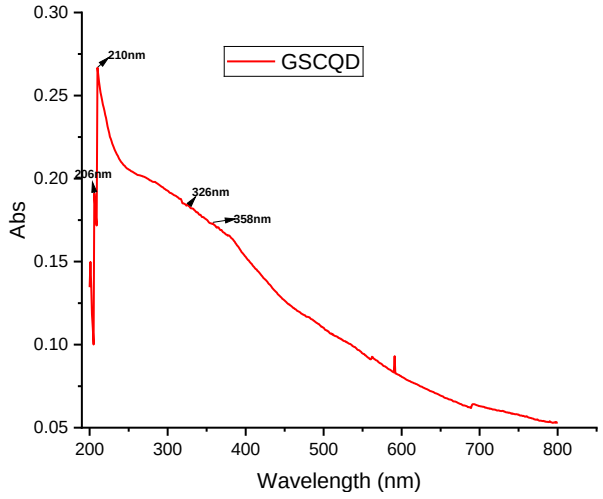

Figure 3. Displayed the UV adsorption peak of GSCQD

The spectrum exhibited a broad absorption band centred at 210 nanometers within the wavelength range of 200 to 800 nanometers, consistent with previous findings reported in [18]. Furthermore, upon exposure to UV light, the aqueous solution of GSCQD displayed green luminescence, as illustrated in Figure 1(b). This emission behaviour is characteristic of CQD synthesis, aligning with the known emission properties of CQDs, which typically emit in the blue, green, and yellow regions [19,20].

3.3. XRD Analysis

X-ray Diffraction (XRD) is a method used to analyze crystal structures by measuring the angles of X-ray diffraction from material lattice planes. When analyzing the groundnut shell-derived carbon quantum dots (GSCQD) and the magnetic iron oxide nanocomposite (GSCQD-$FeFe_2O_4$) (Fig.4) using XRD, there were three peaks at 19.3363, 32.3482, and 38.9350 degrees, indicating the presence of ordered structures in GSCQD. These peaks suggest a degree of crystallinity, and peak broadening, attributed to the small size of carbon quantum dots, implies a reduced crystallite size. Smaller crystallite sizes in nanomaterials result in broader peaks.

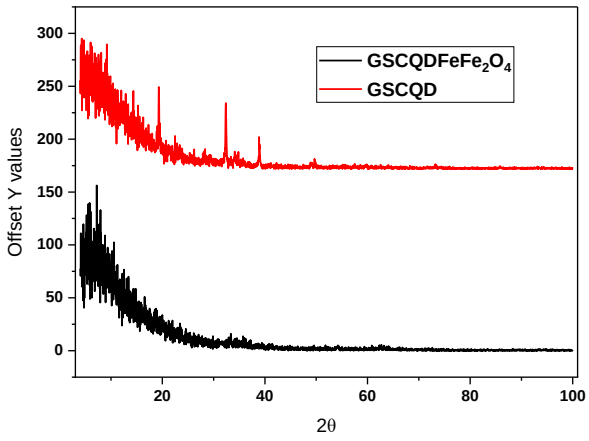

Figure 4. XRD graph for GSCQD-$FeFe_2O_4$ and GSCQD

3.4. Field Emission Scanning Electron Microscope

The nanocomposite, which is composed of carbon quantum dots (CQDs) and magnetic iron oxide nanoparticles, was analyzed using a field emission scanning electron microscope (FE-SEM). The analysis revealed that the CQDs were arranged in clusters, forming cohesive blocks of carbon nanoparticles that made up a significant portion of the CQDs' volume. Fig. 5(a) depicts this clustered arrangement. On the other hand, Fig. 5(b) shows the structure of magnetic iron oxide nanoparticles incorporated into the carbon quantum dot matrix derived from groundnut shells, forming a nanocomposite.

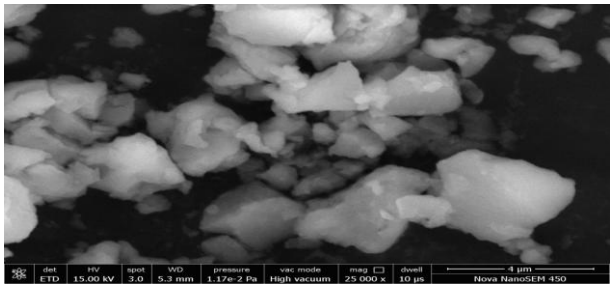

Figure 5(a) FE-SEM Image of GSCQD

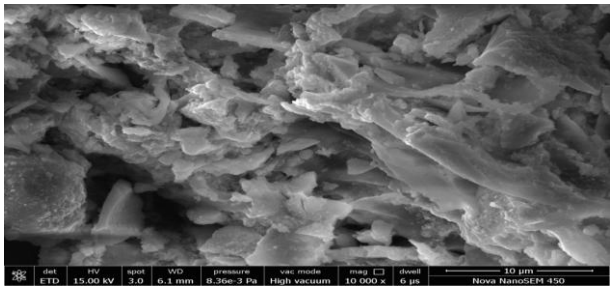

Figure 5(b) FE-SEM Image of GSCQD-$FeFe_2O_4$

3.5. Transmission Electron Microscope

The Transmission Electron Microscopy (TEM) analysis was conducted to investigate the nanoscale dimensions of the adsorbents specifically. According to the findings, carbon quantum dots derived from groundnut shells have a tiny size of only 2 nm (as shown in Fig. 6(a). In general, carbon quantum dots with small particle sizes ranging from 1-10 nm exhibit strong tunable fluorescent properties and highly photo-luminescent emissions. They also contain oxygen-based functional groups and highly desirable properties as semiconductor nanoparticles, which makes them a promising nanomaterials for various applications, including heavy metal detection, adsorption treatment, membrane fabrication, and water pollution treatment [21].

Furthermore, the GSCQDs were utilized to form a nanocomposite by integrating them with magnetic iron oxide nanoparticles (Fig 6(b)). This integration imparts magnetic properties to the resulting nanocomposite, facilitating its retrievability from the remediated solution using external magnetic fields. Consequently, the combination of groundnut shell-derived carbon quantum dots with magnetic iron oxide nanoparticles yields a functional nano-composite capable of efficient adsorption and facile recovery during remediation processes.

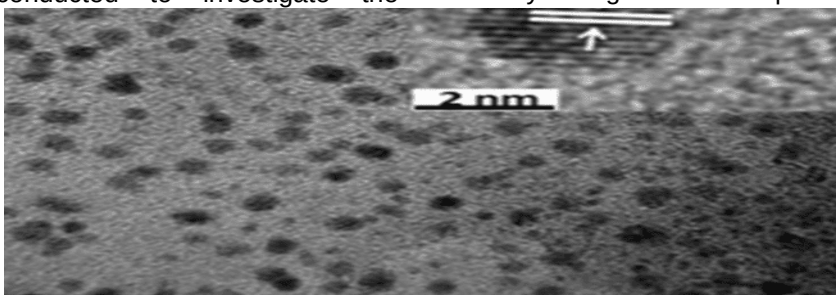

Figure 6(a) TEM Image of GSCQD

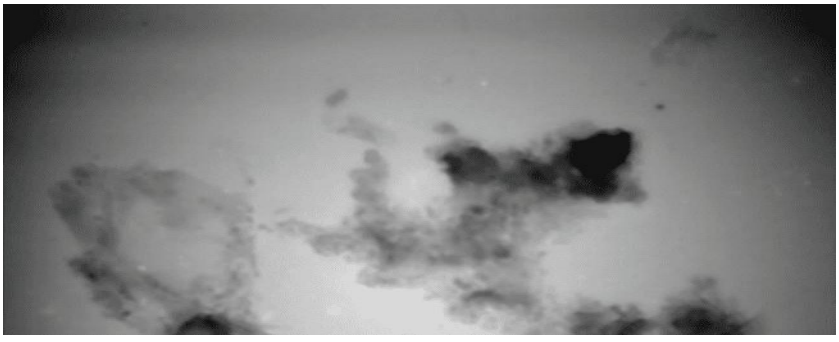

Figure 6(b) TEM Image of GSCQD-$FeFe_2O_4$

3.6. Batch adsorption studies

3.6.1. pH-dependent effect

The pH levels influence the effectiveness of the GSCQD-$FeFe_2O_4$ nanocomposite in eliminating lead ions. The optimal range for removing lead ions is between 5.0 and 6.0 pH (Fig.7), which suggests that the highest efficacy in lead ion removal can be achieved under slightly acidic to neutral conditions. The removal efficiency remains consistent beyond this range, indicating that the nanocomposite is stable within the slightly acidic to neutral pH range. Therefore, it is crucial to maintain the pH within this optimal window to achieve the best results in lead ion removal using the GSCQD-$FeFe_2O_4$ nanocomposite.

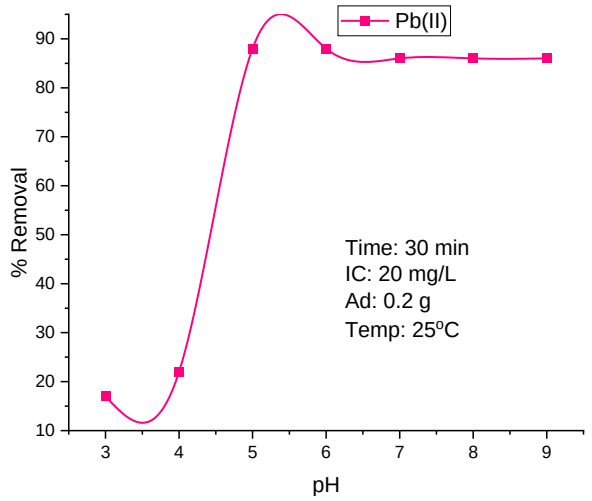

Figure 7. Effect of pH on Pb (II) removal with GSCQD-$FeFe_2O_4$ adsorbent

3.6.2. Effect of Time

The GSCQD-$FeFe_2O_4$ nanocomposite demonstrates an excellent capability for removing lead ions, with the optimal efficiency observed at 20 minutes (Fig. 8). However, it is worth noting that there is a slight reduction in removal efficiency at 25 minutes. This suggests that the nanocomposite requires adequate time for effective adsorption or reaction with lead ions. The plateau or slight decrease in removal efficiency at 25 minutes may be attributed to saturation or other factors influencing the performance of the nanocomposite.

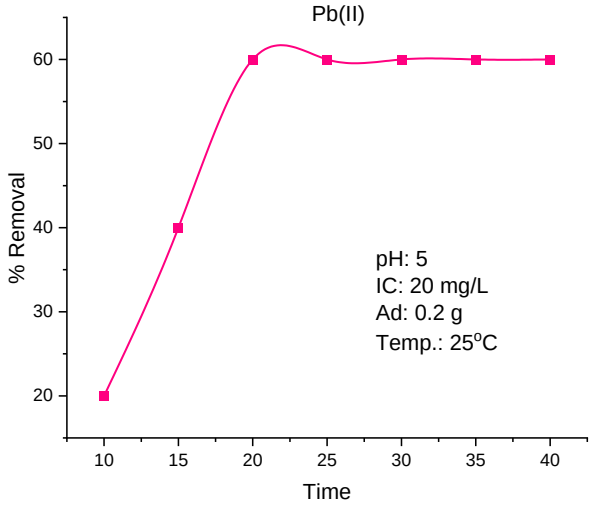

Figure 8. Effect of contact time on Pb (II) removal by GSCQD-$FeFe_2O_4$

3.6.3. Effect of amount of adsorbent

The study aimed to evaluate the adsorption capacity of GSCQD-$FeFe_2O_4$ on lead removal from water. The amount of adsorbent (GSCQD-$FeFe_2O_4$) was varied from 0.1 g to 0.4 g to investigate its impact on adsorption. Other experimental parameters were kept constant to isolate the effect of the amount of adsorbent. The results revealed that the maximum adsorption capacity was achieved at 0.2 g of GSCQD-$FeFe_2O_4$ nanocomposite (Fig. 9). This implies that increasing the amount of adsorbent up to 0.2 g resulted in higher absorption of the target substance. Therefore, it can be inferred that 0.2 g is the optimal or most effective GSCQD-$FeFe_2O_4$ nanocomposite for the given adsorption process under experimental conditions within the tested range.

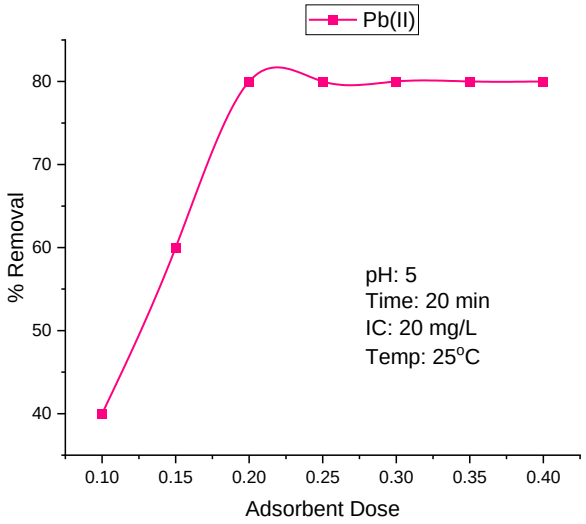

Fig.9 Effect of adsorbent amount on Pb(II) removal by GSCQD-$FeFe_2O_4$

3.6.4. Effect of temperature

The research analyzed the impact of temperature on the adsorption of Pb (II) ions by GSCQD-$FeFe_2O_4$ nanocomposite. The study revealed a decrease in adsorption as the temperature increased from 20°C to 35°C (Fig. 10).

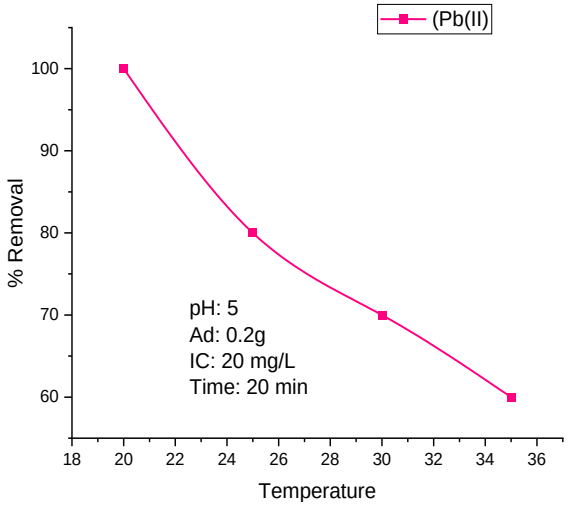

Figure 10. Effect of temperature on Pb(II) removal by GSCQD-$FeFe_2O_4$

When the temperature increases, heavy metal ions are less likely to bind to adsorbents. This is because the higher kinetic energy of the ions weakens the attractive force between them and the adsorbent. As a result, there is a risk of desorption or reduced ion binding, which can lead to a decrease in the stability of the metal ion-adsorbent complex. Other studies on heavy metal ion removal have also reported similar results [22]. Therefore, it is essential to use lower temperatures to achieve efficient adsorption of Pb (II) ions on GSCQD-$FeFe_2O_4$.

3.6.5. Effect of initial concentration of Pb(II)

Adsorption experiments were conducted utilizing GSCQD-$FeFe_2O_4$ for solutions with Pb(II) ion concentrations ranging from 10 mg/L to 70 mg/L. The results depicted in Figure 11 indicate that maximum percentage removal occurred at lower Pb(II) ion concentrations (10 mg/L) and decreased gradually with higher concentrations. At lower concentrations, the binding sites were effectively utilized, leading to approximately 86% adsorption as all metal ions in the solution interacted with these sites.

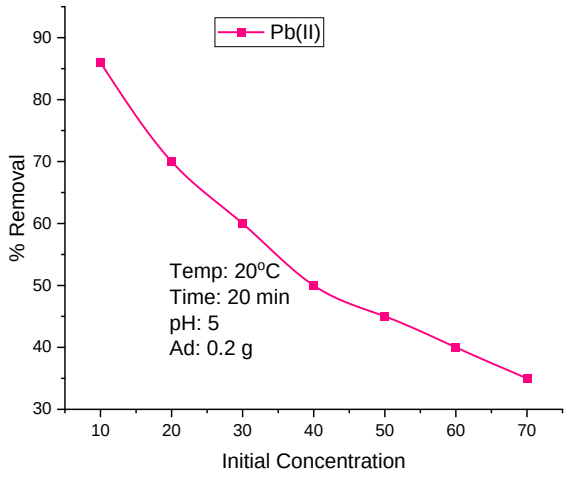

Figure 11. Effect of initial metal ion concentration on Pb(II) removal by GSCQD-$FeFe_2O_4$

3.7. Adsorption isotherms

The Langmuir and Freundlich models are widely used isotherms [23]. Langmuir describes monolayer adsorption, while Freundlich indicates a heterogeneous surface. The linear form of the Langmuir model is expressed as Equation 3.

$$C_e/q_m = 1/K_L q_m + C_e/q_m \qquad (3)$$

The given expression describes the Langmuir adsorption model. It relates the amount of Pb(II) adsorbed per unit of adsorbent (q_e) to the solution's equilibrium concentration (C_e) (Fig 12). The maximum adsorption capacity of the adsorbent is represented by q_m, while K_L denotes the adsorption equilibrium constant.

The Freundlich model suggests that adsorbents have a heterogeneous surface with varying adsorption potential sites. It predicts that the more robust binding sites are occupied first, and the critical strength decreases as the degree of occupation increases. The linear form of the Freundlich adsorption model is expressed by Equation 4.

$$log_{10} q_e = log_{10}(K_f) + (1/n)\, log_{10} C_e \qquad (4)$$

The Freundlich isotherm parameters, K_f (mg/g) and n(mg/L) are essential indicators in understanding the adsorption characteristics of GSCQD-$FeFe_2O_4$ in removing Pb(II) ions from water (Fig 13). These parameters were determined by analyzing the Ce (equilibrium concentration) against $log_{10}q_e$ (amount of adsorbate per unit mass of adsorbent), as presented in Table 1. The model showed a constant of 1.819 and a slope of 1.0697, which indicates favorable adsorption. This is supported by a study that shows values falling within the range of 1 to 10 [24-26]. Both the Langmuir and Freundlich isotherms fitted well with the experimental data, as indicated by high values of the regression coefficient (R^2>0.95). This aligns with a study conducted by Kumar et al., (2019) [27].

Table 1: Langmuir and Freundlich isotherm parameters for the removal of Pb(II) by GSCQD-$FeFe_2O_4$ nanocomposite

Langmuir Parameters	Pb(II)
Q_{max} (mg g^{-1})	37.8
K_L (Lmg^{-1})	12.965
R^2	0.9902
Freundlich Parameters	Pb(II)
K_f (mg g^{-1})	1.819
N (mg L^{-1})	1.0697
R^2	0.9903

Furthermore, the adsorption capacity of 37.8 mg/g was found to be quite good for the removal of Pb(II) from water. The K value of 12.965 suggests strong adsorption of Pb(II) molecules onto the GSCQD-$FeFe_2O_4$ surface, according to Langmuir theory [28].

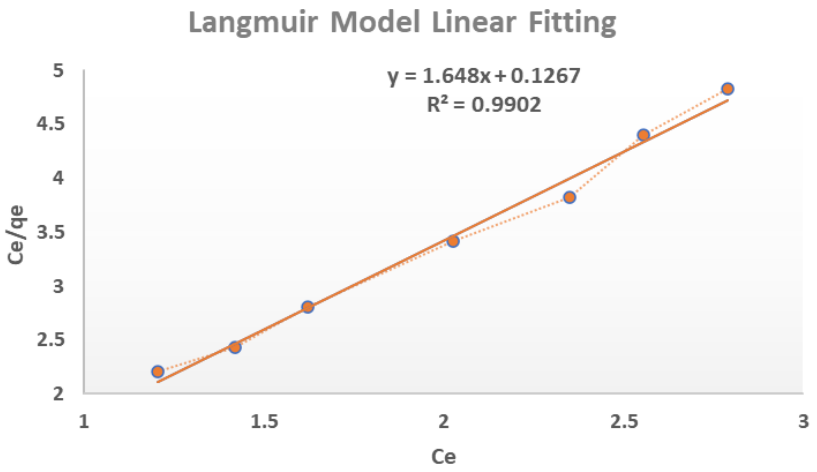

Figure 12. Langmuir isotherm parameter for Pb(II) removal by GSCQD-$FeFe_2O_4$

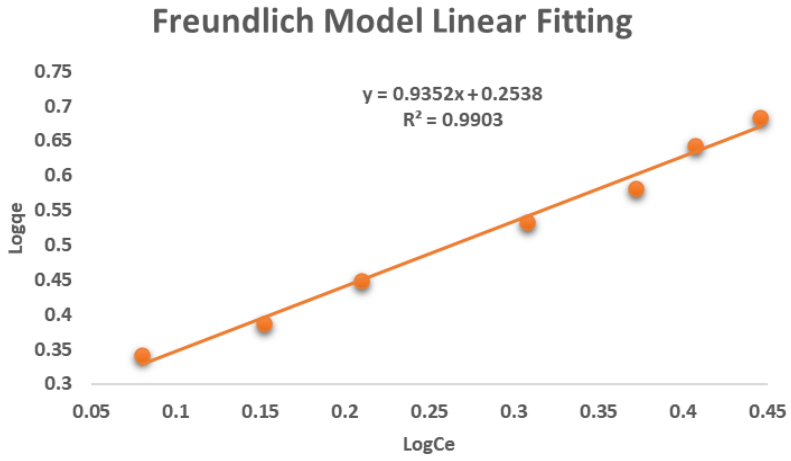

Figure 13. Freundlich Isotherm parameter for Pb(II) removal by GSCQD-$FeFe_2O_4$

3.8. Thermodynamic parameters

The study applied thermodynamic principles to assess the adsorption of Pb(II) by GSCQD-$FeFe_2O_4$. Key thermodynamic parameters, standard Gibbs free energy (ΔG°), standard enthalpy (ΔH°), and standard entropy (ΔS°) were employed for the analysis. The relevant equations were then utilized to compute these thermodynamic parameters.

$$\Delta G = -RTlnk \quad (5)$$

$$\Delta H = -slope\ x\ R \quad (6)$$

$$\Delta S = intercept\ x\ R \quad (7)$$

$$K_L = q_e/c_e \quad (8)$$

The study explores the adsorption behavior of Pb(II) on GSCQD-$FeFe_2O4$ across varying temperatures. Utilizing the universal gas constant (R = 8.314 J mol^{-1} K^{-1}), the temperature (T) in Kelvin, equilibrium concentration (C_e) in milligrams per liter (mg L^{-1}), and the quantity of Pb(II) adsorbed on the surface of GSCQD-$FeFe_2O_4$ (q_e), the investigation examines the relationship between 1/T and the natural logarithm of the adsorption ratio to equilibrium concentration (K_L).

Thermodynamic parameters are derived from the slope and intercept values extracted from the 1/T versus ln(K) graph. Table 2 showcases these parameters, highlighting the negative standard Gibbs free energy (ΔG°) values indicative of spontaneous reactions [29].The manifestation of a negative standard enthalpy (ΔH) signifies the release of exothermic energy during the process of adsorption. This phenomenon aligns with findings documented in a referenced study [30]. Conversely, a positive standard entropy (ΔS) denotes an augmentation in disorder within the system during adsorption, as elucidated in another study [31].

Table 2: Thermodynamic parameters for Pb (II) adsorption by GSCQD-$FeFe_2O_4$ at different temperatures

Heavy Metal	Temperature (K)	K_L	ΔG ($KJmol^{-1}$)	ΔH ($KJmol^{-1}$)	ΔS (JK^{-1} mol^{-1})	R^2
Pb(II)	278	2.205	1.8503	-193.44	75.89	0.99328
	283	2.429	-2.1369			
	288	2.804	-2.4552			
	293	3.415	-23.888			
	298	3.825	-33.7371			
	303	4.401	-37.5508			
	308	4.825	-40.5029			

3.9. Summary

This study aimed to develop a nanocomposite material named "GSCQD-$FeFe_2O_4$" for removing Pb(II) ions from aqueous solutions. The nanocomposite was produced by making carbon quantum dots from groundnut shell material using hydrothermal synthesis and then adding magnetic iron oxide nanoparticles using a straightforward method. The efficiency of the material was tested under various conditions, and its successful synthesis was confirmed through different characterization techniques such as UV-visible spectroscopy, FTIR, XRD, TEM, and FE-SEM.

The study determined the optimal adsorption conditions and found that a monolayer and multilayer adsorption occurred, as confirmed by the R^2 values of both Langmuir and Freundlich models. The maximum adsorption capacity was found to be 37.8 mg/g, indicating that it has good adsorption capacity. Thermodynamic analyses suggested that the adsorption process is spontaneous and exothermic. The GSCQD-$FeFe_2O_4$ nanocomposite was found to be effective in treating wastewater, displaying efficient adsorption capabilities not only for Pb(II) but also for other heavy metals.

Table 3. Comparison of adsorption capacity of GSCQD-$FeFe_2O_4$ with adsorbents used for lead adsorption in different studies

Adsorbent	Adsorption capacity	Model	Ref
Chemical ligand-based Conjugated adsorbent	*172.87 mg/g*	*Langmuir*	*[32]*
Alginate (Alg) caged Magnesium Sulfide Nanoparticle Microbeads	*84.7 mg/g*	*Freundlich*	*[33]*
Activated carbon/alginate/Fe_3O_4 Magnetic Nanocomposite	*37.764 mg/g*	*Freundlich*	*[34]*
Polyethyleneimine-grafted Graphene oxide (PEI/GO)	*64.94 mg/g*	*Freundlich*	*[35]*
MXene/Carbon composite-based Nanofibers (MXene/CNFs membrane	*12.5 mg/g*	*Langmuir*	*[36]*
Groundnut shell carbon quantum dot magnetic iron oxide nanocomposite (GSCQD-$FeFe_2O_4$)	*37.8 mg/g*	Langmuir & Freundlich	*Present study*

4. CONCLUSION

We conducted an investigation to study the adsorption mechanism of Pb(II) ions from aqueous solutions using a nanocomposite material called GSCQD-$FeFe_2O_4$. The material (GSCQD) was synthesized using groundnut shells, which are abundant agricultural waste, showcasing a sustainable approach to waste utilization. The resulting nanocomposite showed significant adsorption capabilities, particularly noteworthy for its ability to eliminate Pb(II) ions. This hazardous heavy metal pollutant Pb(II) is detrimental to human health, even in trace amounts. The magnetic iron oxide nanoparticles and groundnut shell carbon quantum dots (GSCQDs) worked together to facilitate efficient adsorption, with GSCQDs providing active binding sites and the magnetic nanoparticles enabling facile separation. This magnetic feature simplified recovery and reusability, enhancing cost-effectiveness for large-scale water treatment applications.

Various analytical techniques, including UV spectroscopy, FTIR spectroscopy, XRD, TEM, and FE-SEM, were used to characterize the prepared adsorbents, confirming successful synthesis.

Systematic experimentation helped determine optimal conditions for the adsorption process. The pH levels were maintained between 5 and 6, a temperature of 20°C, a contact time of 20 minutes, an adsorbent dosage of 0.2 g, and an initial Pb(II) ions concentration of 10 ppm. Under these optimized parameters, a maximum adsorption efficiency of 86.8% was achieved.

Isotherm studies were conducted to analyze adsorption behavior. Both and Langmuir and Freundlich models provided a better fit for the experimental data confirmed by the R^2 values. The calculated adsorption capacity of 37.8 mg/g was obtained, indicating good adsorption potential. Negative values of Gibbs's free energy (ΔG^o) indicated a spontaneous process, while negative enthalpy change (ΔH^o) suggested exothermic behavior. Conversely, the observed positive entropy change (ΔS^o) indicated an increase in disorder during adsorption, possibly due to desolvation or conformational changes.

The study highlighted the effectiveness of GSCQD-$FeFe_2O_4$ as an adsorbent for Pb(II) ion removal from water. However, further investigations are recommended to assess its reusability and stability under realistic industrial conditions, offering a comprehensive understanding of its potential applications.

Acknowledgment

We thank Dr. Garima Nagpal for her unwavering support and guidance in shaping our study. Gratitude to Sharda University's Central of Instrumentation and Facility for aiding absorbance readings. Special thanks to all contributors for their dedication and collaborative efforts, crucial to the success of this research.

5. REFERENCES

[1] J. Briffa, E. Sinagra, R. Blundell (2020) Heavy metal pollution in the environment and their toxicological effects on humans. *Heliyon.*, *6*(9), e0469. doi.org/10.1016/j.heliyon.2020.

[2] I. Cimboláková, I. Uher, K.V. Laktičová, M. Vargová, T. Kimáková, I. Papajová (2020) Heavy metals and the environment. *Environ. Factors Affect. Hum. Heal.*, *10. book,* doi: 10.5772/intechopen.86876.

[3] A. Jaiswal, A. Verma, P. Jaiswal (2018) Detrimental effects of heavy metals in soil, plants, aquatic ecosystems, and humans. *J. Environ. Pathol. Toxicol. Oncol.*, *37*(3), 183 – 197. doi: 10.1615/JEnvironPatholToxicolOncol.2018025348

[4] B. Dehdashti, M.M. Amin, A. Chavoshani (2020) Other trace elements (heavy metals) and chemicals. *Micropollutants Challenges: Emerging in the Aquatic Environments and Treatment Processes.*, p.*215*. https://www.elsevier.com/books-and-journals

[5] Y.L. Yu, W.Y. Yang, A. Hara, K. Asayama, H.A. Roels, T.S. Nawrot, J.A. Staessen (2023) Public and occupational health risks related to lead exposure updated according to present-day blood lead levels. *Hypertension Research.*, *46*(2), 395-407, doi.org/10.1038/s41440-022-01069-x

[6] M.S. Collin, S.K. Venkatraman, N. Vijayakumar, V. Kanimozhi, S.M. Arbaaz, R.S. Stacey, J. Anusha, R. Choudhary, V. Lvov, G.I. Tovar, F. Senatov (2022) Bioaccumulation of lead (Pb) and its effects on humans: A review. *J. Hazard. Mater. Advances.*, *7*, 100094, doi.org/10.1016/j.hazadv.2022.100094

[7] P. Levallois, P. Barn, M. Valcke, D. Gauvin, T. Kosatsky (2018) Public health consequences of lead in drinking water. *Curr. Environ. Health Rep.*, *5*, 255-262. doi.org/10.1007/s40572-018-0193-0

[8] V. Mohanapriya, R. Sakthivel, N.D.K. Pham, C.K. Cheng, H.S. Le, T.M.H. Dong (2023) Nanotechnology ray of hope for heavy metals removal. *Chemosphere.*, *311*, 136989. doi.org/10.1016/j.chemosphere.2022.136989

[9] S. Ethaib, S. Al-Qutaifia, N. Al-Ansari, S.L. Zubaidi (2022) Function of nanomaterials in removing heavy metals for water and wastewater remediation: A review. *Environments.*, *9*(10), 123. doi.org/10.3390/environments9100123

[10] A. Dhillon, D. Kumar (2019) New generation nano-based adsorbents for water purification. *Nanoscale Materials in Water Purification.,* p.783-798. Elsevier. doi.org/10.1016/B978-0-12-813926-4.00036-7

[11] M. Farshbaf, S. Davaran, F. Rahimi, N. Annabi, R. Salehi, A. Akbarzadeh, (2018) Carbon quantum dots: recent progress on synthesis, surface modification and applications. *Artif. Cells Nanomed. Biotechnol.*, *46*(7), 1331-1348. doi.org/10.1080/21691401.2017.1377725

[12] V.G. Matveeva, L.M. Bronstein (2022) From renewable biomass to nanomaterials: does biomass origin matter? *Prog. Mater. Sci.*, 130, 100999. doi.org/10.1016/j.pmatsci.2022.100999

[13] S. Perumal, R. Atchudan, T.N.J.I. Edison, Y.R. Lee (2021) Sustainable synthesis of multifunctional carbon dots using biomass and their applications: A mini-review. *J. Environ. Chem. Eng.*, *9*(4), 105802. doi.org/10.1016/j.jece.2021.105802

[14] P. Surendran, A. Lakshmanan, G. Vinitha, G.,Ramalingam, P.Rameshkumar (2020) Facile preparation of high fluorescent carbon quantum dots from orange waste peels for nonlinear optical applications. *Luminescence*, *35*(2), 196-202. doi.org/10.1002/bio.3713

[15] V.P. Dinh, N.Q. Tran, Q.H. Tran, T.D. Nguyen (2019) Facile synthesis of $FeFe_2O_4$ magnetic nanomaterial for removing methylene blue from aqueous solution. *Prog. Nat. Sci.: Mater. Int.*, *29*(6), 648-654. doi.org/10.1016/j.pnsc.2019.11.009

[16] H. Asadollahzadeh, M. Ghazizadeh, M. Manzari (2021) Developing a magnetic nanocomposite adsorbent based on carbon quantum dots prepared from Pomegranate peel for the removal of Pb (II) and Cd (II) ions from aqueous solution. *Anal. Methods Environ. Chem. J.*,*4*(03), 33-46. doi.org/10.24200/amecj.v4.i03.149

[17] M.Malacas, M.C.Balberan, N.A.Bederi, C.J.Ramos, M.Rato, A.G.Salazar, E.Roque (2019) The removal of copper (II) and lead (II) from aqueous solution

using Fuller's earth and Fuller's earth-immobilized nanoscale zero-valent iron (FE-NZVI) by adsorption. In *MATEC Web of Conferences* 268, 05006, EDP Sciences. doi.org/10.1051/matecconf/201926805006

[18] R. Qiang, S. Yang, K.Hou, J.Wang (2019) Synthesis of carbon quantum dots with green luminescence from potato starch. *New J. Chem., 43*(27), 10826-10833. doi.org/10.1039/C9NJ02291K

[19] S.D.Pritzl, F.Pschunder, F.Ehrat, S. Bhattacharyya, T.Lohmüller, M.A.Huergo, J.Feldmann (2019) Trans-membrane fluorescence enhancement by carbon dots: ionic interactions and energy transfer. *Nano Letters*, *19*(6), 3886-3891. doi.org/10.1021/acs.nanolett.9b01071

[20] P.Huang, J.Lin, X.Wang, Z.Wang, C.Zhang, M. He, Q.Wang, F.Chen, Z.Li, G.Shen, D.Cui (2012) Light-triggered theranostics based on photosensitizer-conjugated carbon dots for simultaneous enhanced-fluorescence imaging and photodynamic therapy. *Advanced materials (Deerfield Beach, Fla.)*, *24*(37), 5104-5113. doi.org/10.1002%2Fadma.201200650

[21] U.Abd Rani, L.Y.Ng, C.Y.Ng, E. Mahmoudi, (2020) A review of carbon quantum dots and their applications in wastewater treatment. *Adv. colloid Interface Sci.*, *278*, 102124. doi.org/10.1016/j.cis.2020.102124

[22] S.S.Banerjee, M.V.Joshi, R.V.Jayaram (2005) Removal of Cr (VI) and Hg (II) from aqueous solutions using fly ash and impregnated fly ash. *Sep. Sci. Technol.*, *39*(7), 1611-1629. doi.org/10.1081/SS-120030778

[23] H.Zare, H.Heydarzade, M.Rahimnejad, A.Tardast, M.Seyfi, S.M.Peyghambarzadeh (2015) Dried activated sludge as an appropriate biosorbent for the removal of copper (II) ions. *Arab. J. Chem.*, *8*(6), 858-864. doi.org/10.1016/j.arabjc. 2012.11.019

[24] A. Günay, E. Arslankaya, I. Tosun (2007) Lead removal from aqueous solution by natural and pretreated clinoptilolite: adsorption equilibrium and kinetics. *J. Hazard. Mater.*, *146*(1-2), 362-371. doi.org/10.1016/j.jhazmat.2006.12.034

[25] S. Hosseini, M.A. Khan, M.R. Malekbala, W. Cheah, T.S. Choong (2011) Carbon coated monolith, a mesoporous material for the removal of methyl orange from aqueous phase: Adsorption and desorption studies. *Chem. Eng. J.*, *171*(3), 1124-1131. doi.org/10.1016/j.cej.2011.05.010

[26] Y.P.Teoh, M.A.Khan, T.S.Choong (2013) Kinetic and isotherm studies for lead adsorption from aqueous phase on carbon coated monolith. *Chem. Eng. J.*, *217*, 248-255. doi.org/10.1016/j.cej.2012.12.013

[27] P.Kumar, P.Kumar (2019) Removal of cadmium (Cd-II) from aqueous solution using gas industry-based adsorbent. *SN Appl. Sci.*, *1*, 1-8. doi.org/10.1007/s42452-019-0377-8

[28] I.Langmuir (1918) The adsorption of gases on plane surfaces of glass, mica and platinum. *Journal of the J. Am. Chem. Soc.*, *40*(9), 1361-1403. doi.org/10.1021/ja02242a004

[29] S.Mohammadzadeh-Asl, A.Jafari, A. Aghanejad, H. Monirinasab, J.E.N.Dolatabadi (2019) Kinetic and thermodynamic studies of sunitinib malate interaction with albumin using surface plasmon resonance and molecular docking methods. *Microchem. J.*, *150*, 104089. doi.org/10.1016/j.microc.2019.104089

[30] K.P.Yadava, B.S.Tyagi, V.N.Singh (1991) Effect of temperature on the removal of lead (II) by adsorption on China clay and wollastonite. *J. Chem. Technol. Biotechnol.*, *51*(1), 47-60. doi.org/10.1002/jctb.280510105

[31] M.N.Sahmoune (2019) Evaluation of thermodynamic parameters for adsorption of heavy metals by green adsorbents. *Environ. Chem. Lett.*, *17*(2), 697-704. doi.org/10.1007/s10311-018-00819-z

[32] M. M.Hasan, M.S.Salman, M.N. Hasan, A.I. Rehan, M.E. Awual, A.I. Rasee, R.M. Waliullah, M.S. Hossain, K.T. Kubra, M.C. Sheikh, M.A. Khaleque (2023) Facial conjugate adsorbent for sustainable Pb (II) ion monitoring and removal from contaminated water. *Colloids Surf. A: Physicochem. Eng. Asp.*, 673, 131794. doi.org/10.1016/j.colsurfa.2023.131794

[33] M.E.Bidhendi, E.Parandi, M.M.Meymand, H. Sereshti, H.R. Nodeh, S.W. Joo, Y. Vasseghian, N.M. Khatir, S. Rezania (2023) Removal of lead ions from wastewater using magnesium sulfide nanoparticles caged alginate microbeads. *Environ. Res.*, *216*, 114416. doi.org/10.1016/j.envres.2022.114416

[34] K.K.Zadeh, D.Jafari (2023) Activated carbon/alginate/Fe_3O_4 magnetic nanocomposite as a superior functional material for removal of lead from aqueous media. *Biomass Convers. Bior.*, 2023, 1-19. doi.org/10.1007/s13399-023-04040-z

[35] M. Al-Yaari, T.A. Saleh (2023) Removal of Lead from Wastewater Using Synthesized Polyethylene-imine-Grafted Graphene Oxide. *Nanomaterials*, *13*(6), 1078. doi.org/10.3390/nano13061078

[36] I.Mahar, F.K.Mahar, N. Mahar, A.A. Memon, A.A.A. Pirzado, Z. Khatri, K.H. Thebo, A. Ali (2023) Fabrication and characterization of MXene/carbon composite-based nanofibers (MXene/CNFs) membrane: An efficient adsorbent material for removal of Pb^{+2} and As^{+3} ions from water. *Chem. Eng. Res. Des.*, *191*, 462-471. doi.org/10.1016/j.cherd. 2023.02.005

IZVOD

MAGNETNI NANOKOMPOZIT GVOŽĐE-OKSIDA (GSCKD-$FeFe_2O_4$) ZA UKLANJANJE OLOVA IZ VODE

Novi adsorbent, GSCKD-$FeFe_2O_4$, koji kombinuje ugljenične kvantne tačke dobijene iz ljuske kikirikija sa magnetnim nanočesticama oksida gvožđa, sintetizovan je za efikasno uklanjanje Pb(II) iz vode. Studije karakterizacije potvrdile su uspešnu sintezu, sa UV analizom koja je pokazala apsorpciju na 210 nm i zelenom luminiscencijom koja ukazuje na kvantne tačke ugljenika. FT-IR je identifikovao karakteristične funkcionalne grupe, dok je XRD potvrdio dobro uređene strukture. FE-SEM je otkrio grupisane ugljenične nanočestice sa magnetnim oksidom gvožđa, a TEM je pokazao male ugljenične tačke pogodne za adsorpciju. Studije adsorpcije su otkrile optimalne uslove za uklanjanje Pb(II), uključujući pH opseg od 5-6, temperaturu od 20°C, vreme kontakta od 20 minuta i dozu adsorbenta od 0,2 g. Studije izoterme su pokazale da su i Langmuir i Freundlich modeli dobro pristajali, sa izračunatim kapacitetom adsorpcije od 37,8 mg/g. Termodinamička analiza je sugerisala spontanu, egzotermnu adsorpciju sa povećanim poremećajem. GSCKD-$FeFe_2O_4$ je pokazao odličan potencijal za uklanjanje Pb(II), ali su za širu primenljivost potrebna dalja istraživanja o ponovnoj upotrebi i stabilnosti u industrijskim okruženjima.

Ključne reči: *ugljenične kvantne tačke, ljuska kikirikija, magnetna nanočestica gvožđe oksida, olovo, adsorpcioni kapacitet, termodinamički parametri, termodinamičke izoterme*

Naučni rad
Rad primljen: 10.02.2024.
Rad korigovan: 26.02.2024.
Rad prihvaćen: 13.04.2024.
Rad je dostupan na sajtu: www.idk.org.rs/casopis

Fredrick K Saah https://orcid.org/0009-0002-4471-4198
Garima Nagpal https://orcid.org/0000-0002-5182-8233